

MEDL and MEDLA: Methods for Assessment of Scaling by Medians of Log-Squared Nondecimated Wavelet Coefficients

Minkyoung Kang and Brani Vidakovic

H. Milton Stewart School of Industrial & Systems Engineering, Georgia Institute of Technology, 765 Ferst Drive NW, Atlanta, Georgia 30332

Abstract

High-frequency measurements and images acquired from various sources in the real world often possess a degree of self-similarity and inherent regular scaling. When data look like a noise, the scaling exponent may be the only informative feature that summarizes such data. Methods for the assessment of self-similarity by estimating Hurst exponent often involve analysis of rate of decay in a spectrum defined in various multiresolution domains. When this spectrum is calculated using discrete non-decimated wavelet transforms, due to increased autocorrelation in wavelet coefficients, the estimators of H show increased bias compared to the estimators that use traditional orthogonal transforms. At the same time, non-decimated transforms have a number of advantages when employed for calculation of wavelet spectra and estimation of Hurst exponents: the variance of the estimator is smaller, input signals and images could be of arbitrary size, and due to the shift-invariance, the local scaling can be assessed as well. We propose two methods based on robust estimation and resampling that alleviate the effect of increased autocorrelation while maintaining all advantages of non-decimated wavelet transforms. The proposed methods extend the approaches in existing literature where the logarithmic transformation and pairing of wavelet coefficients are used for lowering the bias.

In a simulation study we use fractional Brownian motions with a range of theoretical Hurst exponents. For such signals for which “true” H is known, we demonstrate bias reduction and overall reduction of the mean-squared error by

the two proposed estimators. For fractional Brownian motions, both proposed methods yield estimators of H that are asymptotically normal and unbiased.

Keywords: Non-decimated wavelet transform, scaling, and Hurst exponent

1. Introduction

At first glance, data that scale look like noisy observations, and often the large scale features (basic descriptive statistics, trends, smoothed functional estimates, etc.) carry no useful information. For example, the pupil diameter in humans fluctuates at a high frequency (hundreds of Hz), and prolonged monitoring leads to massive data sets. Researchers found that the high-frequency dynamic of change in the diameter is informative of eye pathologies, e.g., macular degeneration, Moloney et al. (2006). Yet, the trends and traditional summaries of the data are clinically irrelevant, for the magnitude of the diameter depends on the ambient light, and not on the inherent eye pathology.

Our interest focuses on the analysis of self-similar objects. Formally, a deterministic function $f(\mathbf{t})$ of a d -dimensional argument \mathbf{t} is said to be self-similar if $f(\lambda\mathbf{t}) = \lambda^{-H} f(\mathbf{t})$, for some choice of the exponent H , and for all dilation factors λ . The notion of self-similarity has been extended to random processes. Specifically, a stochastic process $\{X(\mathbf{t}), \mathbf{t} \in R^d\}$ is self-similar with scaling exponent (or *Hurst exponent*) H if, for any $\lambda \in R^+$,

$$X(\lambda\mathbf{t}) \stackrel{d}{=} \lambda^H X(\mathbf{t}), \tag{1}$$

where the relation “ $\stackrel{d}{=}$ ” is understood as the equality in all finite dimensional distributions.

In this paper, we are concerned with a precise estimation of scaling exponent H in one-dimensional setting. The results can be readily extended to self-similar objects of arbitrary number of dimensions.

A number of estimation methods for H exist, including: re-scaled range calculation (R/S), Fourier-spectra methods, variance plots, quadratic variations,

zero-level crossings, etc. For a comprehensive description, see Beran (1994), Doukhan et al. (2003), and Abry et al. (2013). Wavelet transforms are especially suitable for modeling self-similar phenomena, as is reflected by vibrant research. An overview is provided in Abry et al. (2000a).

If processes possess a stochastic structure (e.g. Gaussianity, stationary increments), the scaling exponent H becomes a parameter in a well-defined statistical model and can be estimated as such. Fractional Brownian motion (fBm) is important and well understood model for data that scale. Its importance follows from the fact that fBm is a unique Gaussian process with stationary increments that is self-similar, in the sense of (1).

A fBm has a (pseudo)-spectrum of the form $S(\omega) \propto |\omega|^{-(2H+1)}$, and consequently the log-magnitudes of detail coefficients at different resolutions in a wavelet decomposition exhibit a linear relationship. Using non-decimated wavelet domains to leverage on this linearity constitutes the staple of this paper.

Each decomposition level in nondecimated wavelet transform (NDWT) contains the same number of coefficients as the size of the original signal. This redundancy contributes to the accuracy of estimators of H . However, reducing the bias induced by level-wise correlation among the redundant coefficients becomes an important issue. The two estimators we propose are based on the so-called “logarithm-first” approach, connecting Hurst exponent with a robust location and resampling techniques.

The rest of the paper consists of three additional sections and an appendix. Section 2 provides background of wavelet transforms as well as the properties of resulting wavelet coefficients. Section 3 presents distributional results on which the proposed methods are based. Section 4 provides the simulation results and compares the estimation performance of the proposed methods to some standardly used methods. The final Section is reserved for concluding remarks. Appendix contains all technical details for the results presented in Section 3.

2. Orthogonal and non-decimated wavelet transforms

Discrete signals from an acquisition domain can be mapped to the wavelet domain in multiple ways. We overview two versions of discrete wavelet transform: orthogonal wavelet transform (DWT) and non-decimated wavelet transform (NDWT). We also describe algorithmic procedures in performing two versions of wavelet transform and obtaining the wavelet coefficients. Here we focus on functional representations of wavelet transform which is more critical for the subsequent derivations. Interested readers can refer to Nason and Silverman (1995), Vidakovic (1999), and Percival and Walden (2006) for alternative definitions.

Any square-integrable $L_2(\mathbb{R})$ function $f(x)$ can be represented in the wavelet domain as

$$f(x) = \sum_k c_{J_0,k} \phi_{J_0,k}(x) + \sum_{j \geq J_0} \sum_k d_{j,k} \psi_{j,k}(x),$$

where $c_{J_0,k}$ indicates coarse coefficients, $d_{j,k}$ detail coefficients, $\phi_{J_0,k}(x)$ scaling functions, and $\psi_{j,k}(x)$ wavelet functions. We use different decomposing atom functions, as scaling and wavelet functions, depending on a version of wavelet transform. For DWT, the atoms are

$$\begin{aligned} \phi_{J_0,k}(x) &= 2^{J_0/2} \phi(2^{J_0}x - k) \\ \psi_{j,k}(x) &= 2^{j/2} \psi(2^jx - k), \end{aligned}$$

where $x \in \mathbb{R}$, j is a resolution level, J_0 is the coarsest resolution level, and k is the location of an atom.

For NDWT, atoms are

$$\begin{aligned} \phi_{J_0,k}(x) &= 2^{J_0/2} \phi(2^{J_0}(x - k)) \\ \psi_{j,k}(x) &= 2^{j/2} \psi(2^j(x - k)). \end{aligned}$$

Notice that atoms in NDWT have a constant location shift k at all levels, which yields the maximal sampling rate at each level. Two types of coefficients, $c_{J_0,k}$ and $d_{j,k}$, capture coarse and detail fluctuations of an input signal, respectively. These are obtained as

$$\begin{aligned} c_{J_0,k} &= \langle f(x), \phi_{J_0,k} \rangle \\ d_{jk} &= \langle f(x), \psi_{jk} \rangle. \end{aligned}$$

In a p -depth decomposition of an input signal of size m , a NDWT yields $m \times (p + 1)$ wavelet coefficients, while DWT yields m wavelet coefficients independent of p . The redundant transform NDWT decreases the variance of the scaling estimators, but at the same time, increases the correlations among wavelet coefficients. Since the estimators of scaling are based on the second order properties of wavelet coefficients, the NDWT-based estimators can be biased.

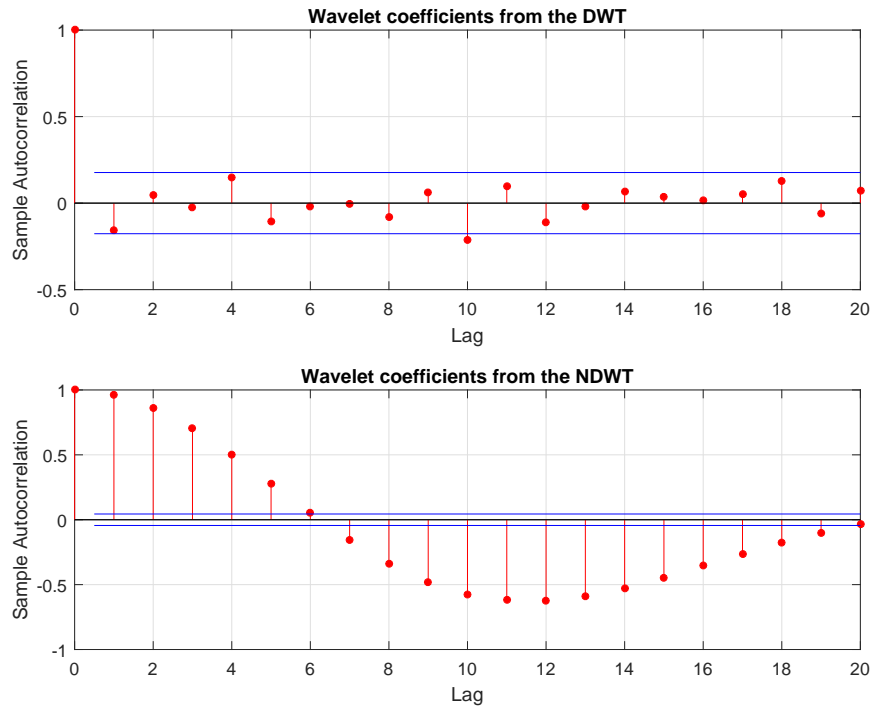


Figure 1: The autocorrelation present in wavelet coefficients from the DWT and the NDWT.

Figure 1 illustrates the autocorrelation within wavelet coefficients in the level $J - 4$ (the level of finest detail is $J - 1$, so $J - 4$ is 4th “most detailed” level) in DWT and NDWT. Haar wavelet was used on a Brownian motion path of size 2^{11} . As we noted before, the coefficients from the NDWT are highly correlated while such correlation is not strong among the DWT coefficients.

The two methods introduced in the following section reduce the effect of correlation among the coefficients, while maintaining redundancy and invariance as desirable threads of NDWT.

3. MEDL and MEDLA Methods

We start by an overview of properties of wavelet coefficients and a brief literature overview methods in literature based on which we develop the proposed methods.

For defining a wavelet spectrum, and subsequently, for estimating H only detail wavelet coefficients are used. When an fBm with Hurst exponent H is mapped to the wavelet domain by DWT, the resulting detail wavelet coefficients satisfy the following properties (Tewfik and Kim, 1992; Abry et al., 1995; Flandrin, 1992):

- (i) d_j , a detail wavelet coefficient at level j , follows the Gaussian distribution with mean 0 and variance $\sigma_0^2 2^{-j(2H+1)}$, where σ_0^2 is the variance of a detail coefficient at level 0,
- (ii) a sequence of wavelet coefficients from level j is stationary, and
- (iii) the covariance between two coefficients from any level of detail decreases exponentially as the distance between them increases; the rate of the decrease depends additionally on the number of vanishing moments of the decomposing wavelet.

From property (i), the relationship between detail wavelet coefficients and Hurst exponent H is

$$\log_2 \mathbb{E}\{d_j^2\} = -j(2H + 1) + 2 \log_2 \sigma_0.$$

Abry et al. (2000b) calculate sample variance of wavelet coefficients to estimate $\mathbb{E}\{d_j^2\}$ assuming i.i.d. Gaussianity of coefficients at level j . Frequently, a squared wavelet coefficient is referred as an “energy.”

Empirically, we look at the levelwise average of squared coefficients (energies),

$$\overline{d_j^2} = \frac{1}{n_j} \sum_{i=1}^{n_j} d_{j,k}^2,$$

where n_j is the number of wavelet coefficients at level j . The relationship

between average energy $\overline{d_j^2}$ and H is

$$\log_2 \overline{d_j^2} \stackrel{d}{\approx} -(2H + 1)j - \log_2 C - \log \chi_{n_j}^2 / \log 2,$$

where $\stackrel{d}{\approx}$ indicates approximate equality in distribution, $\chi_{n_j}^2$ follows a chi-square distribution with n_j degrees of freedom, and C is a constant. The method of Abry et al. (2000b) is affected by the non-normality of $\log_2 \overline{d_j^2}$ and correlation among detail wavelet coefficients, which results in biases of weighted least squares estimates. To reduce the bias, Soltani et al. (2004) defined “mid-energies,” as

$$D_{j,k} = \frac{d_{j,k}^2 + d_{j,k+n_j/2}^2}{2}, k = 1, \dots, n_j/2.$$

According to this approach, each multiresolution level is split on two equal parts and corresponding coefficients from each part are paired, squared, and averaged. This produces a quasi-decorrelation effect. Soltani et al. (2004) show that level-wise averages of $\log_2 D_{j,k}$ are asymptotically normal with the mean $-(2H + 1)j + C$, which is used to estimate H by regression.

The estimators in Soltani et al. (2004) consistently outperform the estimators that use log-average energies, under various settings. Shen et al. (2007) show that the method of Soltani et al. (2004) yields more accurate estimators since it takes the logarithm of a mid-energy, and then averages. Moreover, averaging logged squared wavelet coefficients, rather than taking logarithm of averaged squared wavelet coefficients, is theoretically justified and this approach will be pursued in this paper. For both proposed methods, MEDL and MEDLA, we first take the logarithm of a squared wavelet coefficient or an average of two squared wavelet coefficients, then derive the distribution of such logarithms under the assumption of independence. Next, we use the median of the derived distribution instead of the mean. The medians are more robust to potential outliers that can occur when logarithmic transform of a squared wavelet coefficient is taken and the magnitude of coefficient is close to zero. This numerical

instability may increase the bias and variance of sample means. However, since the logarithms are monotone, the variability of the sample medians will not be affected.

The first proposed method is based on the relationship between the median of the logarithm of squared wavelet coefficients and the Hurst exponent. We use acronym “MEDL” to refer to this method. In MEDL, the logarithmic transform reduces the autocorrelation, while the number of coefficients remains the same. The second method derives the relationship between the median of the logarithm of average of two squared wavelet coefficients and the Hurst exponent. We use acronym “MEDLA” to refer to this method. The MEDLA method is similar in concept to approach of Soltani et al. (2004) who paired and averaged energies prior to taking logarithm. Then the mean of logarithms was connected to H . Instead, we repeatedly sample with replacement m random pairs keeping distance between them at least q_j . Then, as in Soltani et al. (2004) we find the logarithm of pair’s average and connect the Hurst exponent with the median of the logarithms. As we relax the constraints on the distance between energies in each pair, we obtain a larger amount of distinct samples and selecting only N samples out of such sample population further reduces the correlation.

To illustrate the decorrelation effects of the proposed methods, in Figure 2, we compare the autocorrelation present in variables that are averaged: means of d_{jk}^2 for traditional method, means of $\log_2 \left[(d_{jk}^2 + d_{j,k+m/2}^2)/2 \right]$ for Soltani-like method, medians of $\log d_{jk}^2$ for MEDL, and medians of sampled $\log \left[(d_{jk_1}^2 + d_{jk_2}^2)/2 \right]$ for MEDLA method. The two default methods exhibit higher amount of autocorrelation that decreases at a slower rate. The MEDLA shows substantial reduction in correlation.

For formal distributional assessment of the two proposed methods, we start with an arbitrary wavelet coefficient from decomposition level j at location k , d_{jk} , resulting from a non-decimated wavelet transform of a one-dimensional fBm

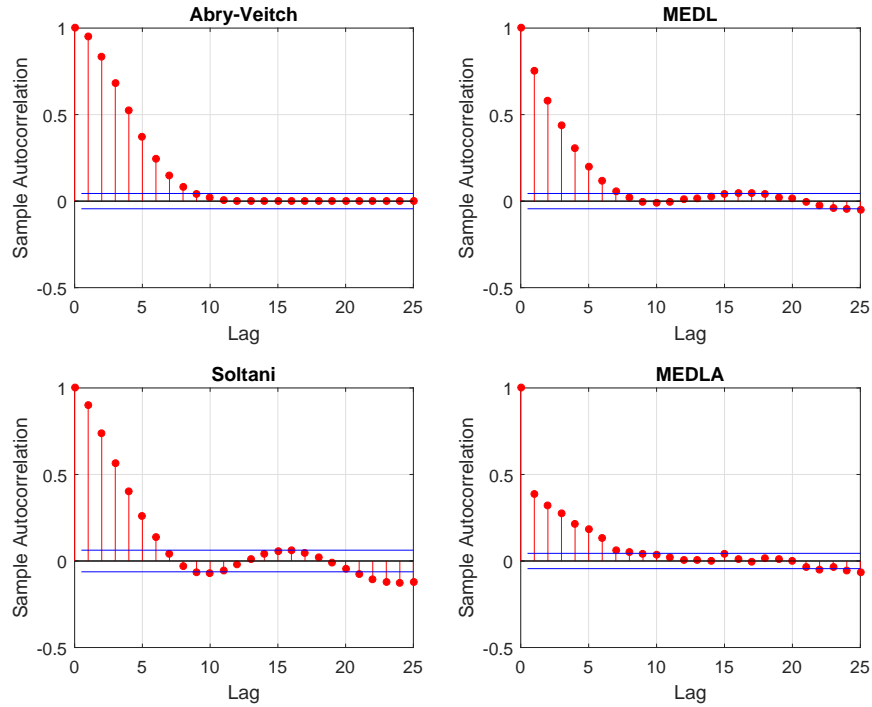


Figure 2: Autocorrelation of variables used in four methods.

$B_H(\omega, t), t \in \mathbb{R}$,

$$d_j = \int_{\mathbb{R}} B_H(\omega, t) \psi_{jk}(t) dt, \text{ for some fixed } k.$$

As Flandrin (1992) showed, the distribution of a single wavelet coefficient is

$$d_j \stackrel{d}{=} 2^{-(H+1/2)j} \sigma Z, \quad (2)$$

where Z follows a standard normal distribution, and σ^2 is the variance of wavelet coefficients at level 0. We will use (2) repeatedly for the derivations that follow.

3.1. MEDL Method

For the median of the logarithm of squared wavelet coefficients (MEDL) method, we derive the relationship between the median of the logarithm on an arbitrary squared wavelet coefficient from decomposition level j and Hurst

exponent H . The following theorem serves as a basis for the MEDL estimator:

Theorem 3.1. *Let y_j^* be the median of $\log d_j^2$, where d_j is an arbitrary wavelet coefficient from level j in a NDWT of a fBm with Hurst exponent H . Then, the population median is*

$$y_j^* = -\log 2 (2H + 1)j + C, \quad (3)$$

where C is a constant independent of j . The Hurst exponent can be estimated as

$$\widehat{H} = -\frac{\widehat{\beta}}{2 \log 2} - \frac{1}{2}, \quad (4)$$

where $\widehat{\beta}$ is the slope in ordinary least squares (OLS) linear regression on pairs (j, \widehat{y}_j^*) , and \widehat{y}_j^* is the sample median.

The proof of Theorem 3.1 is deferred to Appendix A. We estimate y_j^* by taking sample median of logged energies at each level. The use of OLS linear regression is justified by the fact that variances of the sample medians \widehat{y}_j^* are constant in j , that is,

Lemma 3.1. *The variance of sample median \widehat{y}_j^* at level j is approximately*

$$\frac{\pi e^Q}{2NQ},$$

where N is the sample size and $Q = (\Phi^{-1}(3/4))^2$.

The theorem is stating that the logarithm acts as a variance stabilizing operator; the variance of the sample median is independent of level j , and ordinary regression to find slope β in Theorem 3.1 is fully justified. Note that the use of OLS regression is not adequate in DWT; the weighted regression is needed to account for levelwise heteroscedasticity.

The levelwise variance is approximately $5.4418/N$, independent of H and σ^2 . The proof of Theorem 3.1 is deferred to Appendix A. In addition, for \widehat{H} the

normal approximation applies:

Theorem 3.2. *The MEDL estimator \hat{H} follows the asymptotic normal distribution*

$$\hat{H} \stackrel{approx}{\sim} \mathcal{N}\left(H, \frac{3A}{Nm(m^2 - 1)(\log 2)^2}\right),$$

where $A = \pi e^Q / (2Q) \cong 5.4418$, N is the sample size, and m is the number of levels used in the spectrum.

The proof of Theorem 3.2 is deferred to Appendix A. To illustrate Theorem 3.2, we perform an NDWT of depth 10 on simulated fBm's with $H = 0.3, 0.5$, and 0.7 . We use resulting wavelet coefficients from levels $J-7$ to $J-2$ inclusive (i.e., six levels) to estimate H with MEDL. Following Theorem 3.2, \hat{H} of MEDL in the simulation follows a normal distribution with mean H and variance 7.9007×10^{-5} , which is illustrated in Figure 3.

3.2. MEDLA Method

For the median of the logarithm of averaged squared wavelet coefficients (MEDLA) method, we derive the relationship between logarithm of an average of two energies and Hurst exponent H . Soltani et al. (2004) proposed a method that quasi-decorrelates wavelet coefficients by splitting all wavelet coefficients from one level into left and right sections and pairing every coefficient in the left section with its counterpart in the right section, maintaining an equal distance to its pair (i.e., members in each pair are $m/2$ apart when m is the number of wavelet coefficients on that level). Then, Soltani et al. (2004) averaged every pair of energies and took logarithm of each average. We follow similar idea except that instead of fixing the combinations of pairs, which amounts to $m/2$ pairs in Soltani et al. (2004), we randomly sample with replacement m pairs whose members are at least q_j apart. Based on sample autocorrelation graphs, we define $q_j = 2^{J-j}$ that decrease with level j because the finer the subspace (i.e., larger j), the lower the correlation among wavelet coefficients. Then, we propose an estimator of H based on the following result.

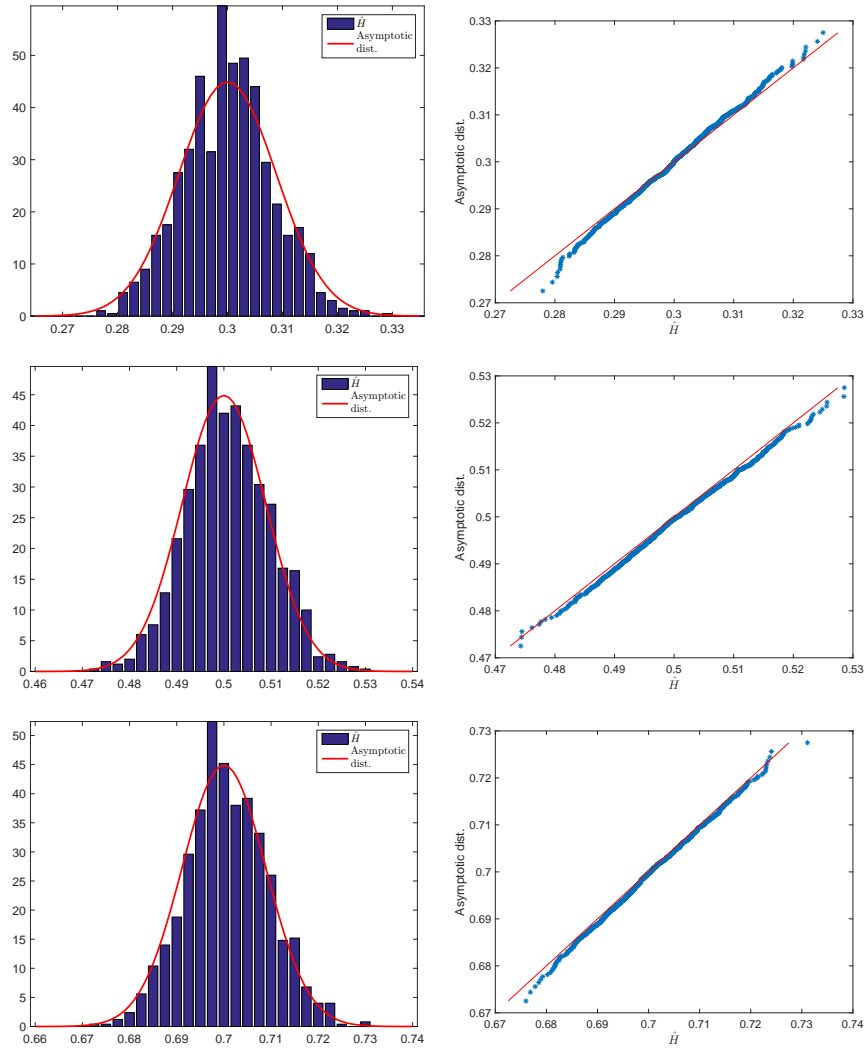


Figure 3: Panels on the right are histograms of \hat{H} and panels on the left are q-q plots of \hat{H} versus the quantiles asymptotic distribution when $H = 0.3, 0.5$, and 0.7 , respectively.

Theorem 3.3. *Let d_{jk_1} and d_{jk_2} be two wavelet coefficients from level j , at positions k_1 and k_2 , respectively, from a NDWT of a fBm with Hurst exponent H . Assume that $|k_1 - k_2| > q_j$, where q_j is the minimum separation distance that depends on level j and selected wavelet base. Let y_j^* be the median of $\log \left[\frac{d_{jk_1}^2 + d_{jk_2}^2}{2} \right]$. Then, as in Theorem 3.1, results (3) and (4) hold.*

The proof of Theorem 3.3 is deferred to Appendix B. To estimate y_j^* , we first repeatedly sample m pairs of wavelet coefficients with replacement from all pairs that are at least q_j apart. Then, we take logarithm of pair's average energy and take the median. As in Theorem 3.1, the variances of sample medians \hat{y}_j^* are free of j .

Lemma 3.2. *The variance of the sample median \hat{y}_j^* at level j is approximated by*

$$\frac{1}{N(\log 2)^2},$$

where N is the sample size.

The proof is straightforward and given in Appendix B. Thus, the variance of \hat{y}_j^* is constant over levels. We find that MEDLA estimator of H indeed follows a approximately normal distribution with a mean and a variance given in the following theorem.

Theorem 3.4. *The estimator \hat{H} of MEDLA follows the asymptotic normal distribution*

$$\hat{H} \stackrel{approx}{\sim} \mathcal{N} \left(H, \frac{3}{Nm(m^2 - 1)(\log 2)^4} \right),$$

where N is the sample size, and m is the number of levels used in the spectrum.

The proof of Theorem 3.4 is deferred to Appendix B. To illustrate Theorem 3.4, we use the same wavelet coefficients from the simulation in section 3.1. Following Theorem 3.4, \hat{H} of MEDLA in the simulation follows an approximate

normal distribution with mean H and variance 7.9007×10^{-5} , which is shown in Figure 4.

4. Simulations

Next, we assess the performance of MeDL and MEDLA in estimation of Hurst exponent. We simulate three sets of three hundred one-dimensional fractional Brownian motion (1-D fBm) paths of size 2^{11} with Hurst exponents 0.3, 0.5, and 0.7 respectively. Then, we perform an NDWT of depth 10 with a Haar wavelet on each simulated signal and obtain wavelet coefficients to which we apply MEDL and MEDLA. For all methods and estimations, we use wavelet coefficients from levels $J - 7$ to $J - 2$ in the regression. We compare the estimation performance of the proposed methods to two standard methods: a method of Veitch and Abry (1999) and a method of Soltani et al. (2004), both in the context of NDWT. We present the estimation performance in terms of mean, variance, bias-squared, and mean squared error, based on 300 simulations for each case. Table 1 and Figure 5 indicate that as H increases, the proposed methods outperform the standard methods. For smaller H , the estimation performance of all methods is comparable.

5. Conclusions

We proposed two methods for robust estimation of Hurst exponent in one- and two-dimensional signals that scale. Unlike the standard methods, the proposed methods are based on NDWT. The motivation for using NDWT was its redundancy and time-invariance. However, the redundancy, which was useful for the stability of estimation, increases autocorrelations among the wavelet coefficients. The proposed methods lower the present autocorrelation by (i) taking logarithm of the squared wavelet coefficients prior to averaging, (ii) relating the Hurst exponent to the median of the model distribution, rather than the mean, and (iii) resampling the coefficients.

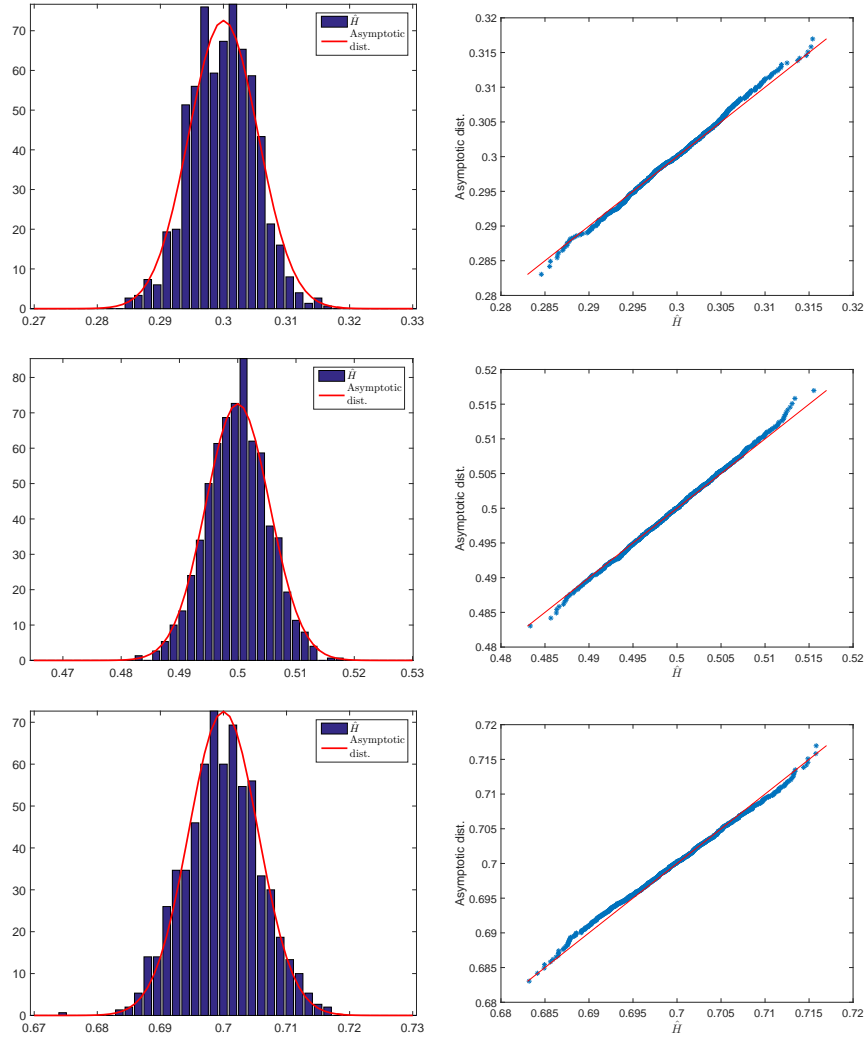
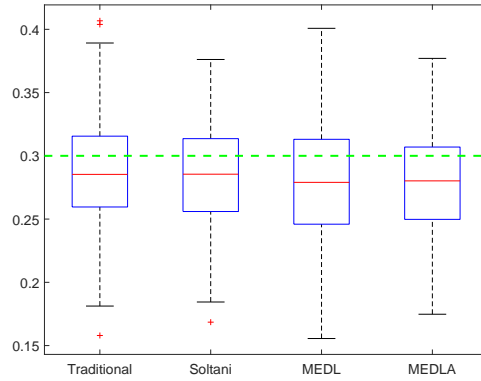
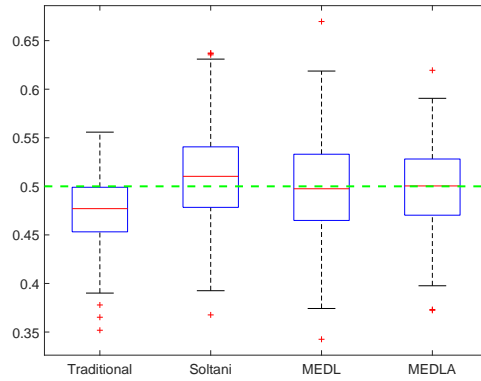


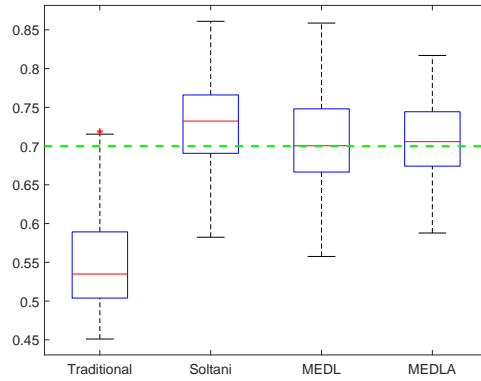
Figure 4: Panels on the right are histograms of \hat{H} and panels on the left are q-q plots of \hat{H} versus the quantiles of asymptotic distribution when $H = 0.3, 0.5$, and 0.7 , respectively.



(a) $H=0.3$



(b) $H=0.5$



(c) $H=0.7$

Figure 5: Boxplots of \hat{H} by four methods with 300 simulated 1-D fBm signals of size 2^{11} when $H=0.3, 0.5,$ and 0.7

$H=0.3$

Method	Traditional	Soltani	MEDL	MEDLA
Mean	0.2864	0.2849	0.2778	0.2783
Variance	0.0017	0.0015	0.0021	0.0016
Bias-squared	0.0002	0.0003	0.0005	0.0005
MSE	0.0019	0.0018	0.0026	0.0021

$H=0.5$

Method	Traditional	Soltani	MEDL	MEDLA
Mean	0.475	0.5091	0.4966	0.4982
Variance	0.0012	0.0022	0.0023	0.0017
Bias-squared	0.0006	6.7E-5	4.1E-6	1.3E-6
MSE	0.0018	0.0023	0.0023	0.0017

$H=0.7$

Method	Traditional	Soltani	MEDL	MEDLA
Mean	0.5524	0.7286	0.7065	0.7084
Variance	0.0039	0.0028	0.0033	0.0024
Bias-squared	0.0217	0.0008	3.3E-5	6.2E-5
MSE	0.0256	0.0036	0.0033	0.0024

Table 1: Estimation of H with 300 simulated 1-D fBm signals of size 2^{11} when $H=0.3, 0.5$, and 0.7 by four methods

The methods are compared to standard approaches and give estimators with smaller MSE for a range of input conditions.

Instead of medians in (ii) we could employ any other quantile; the methodology is equivalent and will differ for the intercept and variance in the regressions.

References

References

Abry P, Flandrin P, Taqqu M, Veitch D. Wavelets for the analysis, estimation, and synthesis of scaling data. In: Park K, Willinger W, editors. Self-Similar Network Traffic and Performance Evaluation. Wiley; 2000a. p. 39–88.

Abry P, Flandrin P, Taqqu MS, Veitch D. Wavelets for the analysis, estimation and synthesis of scaling data. Self-similar network traffic and performance evaluation 2000b;:39–88.

- Abry P, Gonçalves P, Flandrin P. Wavelets, spectrum analysis and 1/f processes. In: Wavelets and statistics. Springer; 1995. p. 15–29.
- Abry P, Gonçalves P, Vehe J. Scaling, Fractals and Wavelets. Wiley-ISTE, 2013.
- Beran J. Statistics for Long-memory Processes. Chapman & Hall, 1994.
- Doukhan P, Oppenheim G, Taqqu MS. Theory and Applications of Long-range Dependence. Springer Science & Business Media, 2003.
- Flandrin P. Wavelet analysis and synthesis of fractional brownian motion. Information Theory, IEEE Transactions on 1992;38(2):910–7.
- Moloney KP, Jacko JA, Vidakovic B, Sainfort F, Leonard VK, Shi B. Leveraging data complexity: Pupillary behavior of older adults with visual impairment during hci. Journal ACM Transactions on Computer-Human Interaction (TOCHI) 2006;13(3):376–402.
- Nason GP, Silverman BW. The stationary wavelet transform and some statistical applications. Lecture Notes in Statistics 103: Wavelets and Statistics 1995;:281–99.
- Percival DB, Walden AT. Wavelet methods for time series analysis. volume 4. Cambridge university press, 2006.
- Shen H, Zhu Z, Lee TC. Robust estimation of the self-similarity parameter in network traffic using wavelet transform. Signal Processing 2007;87:2111–24.
- Soltani S, Simard P, Boichu D. Estimation of the self-similarity parameter using the wavelet transform. Signal Processing 2004;84(1):117–23.
- Tewfik AH, Kim M. Correlation structure of the discrete wavelet coefficients of fractional brownian motion. IEEE transactions on information theory 1992;38(2):904–9.

Veitch D, Abry P. A wavelet-based joint estimator of the parameters of long-range dependence. *Information Theory, IEEE Transactions on* 1999;45(3):878–97.

Vidakovic B. *Statistical Modeling by Wavelets*. John Wiley & Sons, 1999.

Appendix

A. Derivation of MEDL

Proof of Theorem 3.1

A single wavelet coefficient in a non-decimated wavelet transform of fBm(H) is normally distributed, with variance depending on its level j ,

$$d_j \stackrel{d}{=} \mathcal{N}(0, 2^{-(2H+1)j}\sigma^2).$$

Its rescaled energy is χ^2 with one degree of freedom,

$$\delta = \frac{2^{(2H+1)j}}{\sigma^2} d_j^2 \stackrel{d}{=} \chi_1^2,$$

with density

$$\frac{\delta^{1/2-1}(\frac{1}{2})^{1/2}}{\Gamma(\frac{1}{2})} e^{-\delta/2} = \frac{e^{-\delta/2}}{\sqrt{2\delta}\Gamma(\frac{1}{2})}.$$

The pdf of d_j^2 is

$$f(d_j^2) = \frac{e^{-c_j d_j^2/2}}{\sqrt{2c_j d_j^2} \Gamma(1/2)} c_j,$$

where $c_j = \frac{2^{(2H+1)j}}{\sigma^2}$. Let $y = \log d_j^2$, then $d_j^2 = e^y$ and $\frac{\partial d_j^2}{\partial y} = e^y$. The pdf of y is

$$f(y) = \frac{c_j e^{-\frac{c_j e^y}{2}}}{\sqrt{2c_j e^y} \Gamma(1/2)} e^y = \frac{\sqrt{c_j} e^{-\frac{c_j e^y}{2}} e^{y/2}}{\sqrt{2}\Gamma(1/2)} = \sqrt{\frac{c_j}{2\pi}} e^{-\frac{c_j e^y}{2}} e^{y/2},$$

The cdf of y is

$$F(y) = \int_{-\infty}^y f(t)dt = 2\Phi\left(\sqrt{c_j}e^{y/2}\right) - 1,$$

where Φ is the cdf of standard normal distribution. Let y^* be the median of the distribution of y . We obtain the expression of y^* by solving $F(y^*) = 1/2$. This results in

$$y^* = 2 \log \left[\frac{1}{\sqrt{c_j}} \Phi^{-1}(3/4) \right]$$

From this equation, we can find a link between y^* and the Hurst exponent H by substituting c_j ,

$$\begin{aligned} y^* &= 2 \log[\Phi^{-1}(3/4)] - \log c_j \\ &= -\log 2 (2H + 1)j + \log \sigma^2 + 2 \log[\Phi^{-1}(3/4)] \\ &= -\log 2 (2H + 1)j + C, \end{aligned} \tag{5}$$

where C is a constant independent on the level j .

Proof of Lemma 3.1

An approximation of variance of sample median \hat{y}_j^* is obtained using normal approximation to a quantile of absolutely continuous distributions,

$$Var(\hat{y}_j^*) \approx \frac{1}{4N(f(y_j^*))^2}.$$

After substituting the expression for y^* we obtain Lemma 3.1

$$Var(\hat{y}_j^*) \approx \frac{\pi e^Q}{2NQ}, \quad Q = [\Phi^{-1}(3/4)]^2 \approx 0.4549.$$

Thus the variance of the sample median is approximately $5.4418/N$.

Proof of Theorem 3.2

An NDWT-based spectrum uses the pairs

$$(j, \hat{y}_j^*), \quad j = J - m - a - 1, \dots, J - a - 1.$$

from m decomposition levels, starting with a coarse $j = J - m - a$ level and ending with finer level $j = J - 1 - a$. Here a is an arbitrary integer between 0 and $J - 3$. When $a = 0$, the finest level $j = J - 1$ until level $J - 1 - m$ are used.

Then the spectral slope is

$$\hat{\beta} = \frac{12}{m(m^2 - 1)} \sum_{j=J-m-a-1}^{J-1-a} (j - J - a - (m + 1)/2) \hat{y}_j^*.$$

The estimator $\hat{\beta}$ is unbiased,

$$\begin{aligned} E\hat{\beta} &= \frac{12}{m(m^2 - 1)} \sum_{j=J-m-a-1}^{J-1-a} (j - J - a - (m + 1)/2) (-\log 2 (2H + 1)j + C) \\ &= -\log 2 (2H + 1), \end{aligned}$$

where C is a constant and H is the theoretical Hurst exponent.

By substituting $\text{Var}(\hat{y}_j^*) = A/N$ from Theorem 3.1 we find

$$\text{Var}(\hat{\beta}) = \frac{12A}{Nm(m^2 - 1)}, \quad \text{and} \quad \text{Var}(\hat{H}) = \frac{3A}{Nm(m^2 - 1)(\log 2)^2},$$

for $\hat{H} = -\hat{\beta}/(2 \log 2) - 1/2$.

Thus, the MEDL estimator \hat{H} is approximately normal with mean H and variance $3A/(Nm(m^2 - 1)(\log 2)^2)$, where $A \cong 5.4418$, N is the sample size, and m is the number of levels used for the spectrum.

B. Derivation of MEDLA

Proof of Theorem 3.3.

We begin by selecting the pair of wavelet coefficients that follow a normal distribution with a zero mean and a variance dependent on level j , from which the

wavelet coefficients are sampled.

$$d_{j,k_1}, d_{j,k_2} \sim \mathcal{N}(0, 2^{-(2H+1)j} \sigma^2),$$

where σ is the standard deviation of wavelet coefficients from level 0, k_1 and k_2 are positions of wavelet coefficients in level j , and H is the Hurst exponent. We also assume that coefficients d_{j,k_1} and d_{j,k_2} are independent, which is a reasonable assumption when the distance $|k_1 - k_2| > q_j = 2^{J-j}$. Then, we define δ as

$$\delta = \frac{2^{(2H+1)j}}{\sigma^2} (d_{j,k_1}^2 + d_{j,k_2}^2) = C_j \cdot a,$$

for $C_j = \frac{2 \cdot 2^{(2H+1)j}}{\sigma^2}$ and $a = \frac{d_1^2 + d_2^2}{2}$. Since δ follow χ_2^2 distribution, the pdf of the average of two squared wavelet coefficients a is

$$f(a) = \frac{C_j}{2} e^{-\frac{C_j a}{2}}.$$

Denote $y = \log a$. The pdf and cdf of y are

$$\begin{aligned} f(y) &= \frac{C_j}{2} e^{-\frac{C_j e^y}{2}} e^y \\ F(y) &= 1 - e^{-C_j e^y / 2}. \end{aligned}$$

Let y^* be the median of y . The expression for y^* is obtained by solving $F(y^*) = 1 - e^{-C_j e^{y^*} / 2} = 1/2$,

$$y^* = \log(\log 4) - \log C_j.$$

After replacing C_j with $\frac{2 \cdot 2^{(2H+1)j}}{\sigma^2}$, the median becomes

$$y^* = -\log 2 (2H + 1)j + \log \sigma^2 + \log(\log 2),$$

similarly as in (5) in the MEDL method.

Proof of Lemma 3.2

An approximation of variance of sample median is obtained as

$$\text{Var}(\hat{y}_j^*) \approx \frac{1}{4n(f(y_j^*))^2}.$$

After plugging in the expression for y^* into $\frac{1}{4n(f(y_j^*))^2}$, we obtain

$$\text{Var}(\hat{y}_j^*) \approx \frac{1}{N(\log 2)^2},$$

Thus the variance of the sample median in MEDLA method is approximately $2.08/N$.

Proof of Theorem 3.4

For the distribution of \hat{H} from MEDLA, we follow the same regression steps on pair (j, \hat{y}_j^*) as in Appendix A. By substituting $\text{Var}(\hat{y}_j^*) = \frac{1}{N(\log 2)^2}$ from (3.2) we find

$$\text{Var}(\hat{\beta}) = \frac{12}{Nm(m^2 - 1)(\log 2)^2}, \text{ and } \text{Var}(\hat{H}) = \frac{3}{Nm(m^2 - 1)(\log 2)^4},$$

for $\hat{H} = -\hat{\beta}/(2 \log 2) - 1/2$. Thus, the MEDLA estimator \hat{H} is approximately normal with mean H and variance $3/(Nm(m^2 - 1)(\log 2)^2)$, where N is the sample size, and m is the number of levels used for the spectrum.